Anti-neuropilin-1 monoclonal antibody suppresses the migration and invasion of human gastric cancer cells via Akt dephosphorylation

YUAN DING[1*], JUAN ZHOU[1*], SHENGYU WANG[2], YUE LI[1], YANJUN MI[1], SHIHUA GAO[1], YUN XU[1], YUQIANG CHEN[1] and JIANGHUA YAN[2]

[1]Department of Oncology, The 174th Hospital of The Chinese People's Liberation Army, The Affiliated Chenggong Hospital of Xiamen University, Xiamen, Fujian 361003; [2]Cancer Research Center, Medical College of Xiamen University, Xiamen, Fujian 361102, P.R. China

Received January 24, 2016; Accepted February 24, 2017

DOI: 10.3892/etm.2018.6234

Abstract. Neuropilin-1 (NRP-1) is involved in a range of physiological and pathological processes, including neuronal cell guidance, cardiovascular development, immunity, angiogenesis and the pathogenesis of cancer. Targeting of NRP-1 is considered to be a potential cancer therapy and a number of approaches have been investigated, including the use of small interfering RNA, peptides, soluble NRP antagonists and monoclonal antibodies. The present study used a novel anti-neuropilin-1 monoclonal antibody (anti-NRP-1 mAb) to investigate its potential anti-tumor effects on human gastric cancer cells *in vitro* and *in vivo*, as well as its underlying mechanisms of action. Using an MTT assay, it was observed that anti-NRP-1 mAb (<150 μg/ml) had no effects on the viability of gastric cancer cell line BGC-823, while a Boyden chamber assay indicated that treatment with anti-NRP-1 mAb suppressed the migration and invasion of BGC-823 cells. Western blot analysis also demonstrated that phosphorylation of Akt was reduced in BGC-823 cells treated with anti-NRP-1 mAb. Furthermore, anti-NRP-1 mAb suppressed the growth of gastric cancer xenograft tumors and downregulated the expression of vascular endothelial growth factor proteins within tumors in nude mice. These data indicate the potential effects of anti-NRP-1 mAb on malignant tumors and suggest that inhibition of NRP-1 function with anti-NRP-1 mAb may be a novel therapeutic approach in the treatment of cancer.

Correspondence to: Professor Yuqiang Chen, Department of Oncology, The 174th Hospital of The Chinese People's Liberation Army, The Affiliated Chenggong Hospital of Xiamen University, 94-96 Wenyuan Road, Xiamen, Fujian 361003, P.R. China
E-mail: chenyq7070@163.com

Professor Jianghua Yan, Cancer Research Center, Medical College of Xiamen University, Xiang'an South Road, Xiamen, Fujian 361102, P.R. China
E-mail: jhyan@xmu.edu.cn

*Contributed equally

Key words: neuropilin-1, antibody, gastric cancer, migration, invasion, vascular endothelial growth factor

Introduction

Neuropilin (NRP) was first identified as a single-pass transmembrane protein from the optic tract of *Xenopus laevis* in 1987 (1). In 1997, two separate groups used a genetic expression-cloning technique to characterize NRP-1 as the receptor for semaphorin (sema)-3A during development of the nervous system (2-4). NRP-1 consists of an 860-amino acid (aa) extracellular glycoprotein region, a 22-aa transmembrane region and a 40-aa intracellular region. The extracellular region consists of the following five domains; A meprin, A-5 protein and mu (MAM) domain at its C-terminus, two complement-binding-like (CUB) domains (a1 and a2), and two coagulation factor V/VIII homology-like domains (b1 and b2) (5). The MAM domain is considered to mediate dimerization of NRP1, while the a1/a2 and b1/b2 domains aid binding to class 3 semaphorins and vascular endothelial growth factor (VEGF) proteins, respectively (6,7). These binding activities enable NRP-1 to function as a coreceptor that enhances responses to a number of growth factors and mediators, including sema-3A and the 165-aa variant of VEGF. Therefore, NRP-1 is involved in a range of physiological and pathological processes, including neuronal guidance, cardiovascular development, immunity, angiogenesis and the pathogenesis of cancer (8,9).

NRP-1 is expressed on plasmacytoid dendritic cells (10-12), arterial endothelial cells (13) and a small subset of T regulatory cells found in lymphoid tissue (14). Recently, the roles of NRP-1 as a mediator of tumor development and progression have been investigated, due to observations that NRP-1 is expressed extensively in tumor cells, including colon cancer, breast cancer, lung cancer and glioma cells and vasculatures (15-20) and the association between NRP1 overexpression with tumor progression and poor clinical outcome (9,21). Thus, expression

of NRP-1 may be a diagnostic and prognostic marker of malignant tumors (22,23).

Targeting of NRP-1 is considered to be a potential cancer therapy and a number of current methods aim to inhibit the oncogenic activities of NRP-1, including small interfering RNA (17,24-26), peptides (27-30), soluble NRP antagonists (17,31), monoclonal antibodies (mAbs) (32) and other small molecule inhibitors (17,33-38). Preclinical data has indicated that inhibition of NRP1 suppresses tumor growth by preventing angiogenesis, in addition to directly inhibiting tumor cell proliferation in certain models (including, non-small cell lung cancer (NSCLC) and glioma), thus demonstrating the potential of NRP-1 targeting in anti-angiogenic and antitumor therapies (23,39). As monoclonal antibodies have a number of advantages, including high specificity and strong affinity, further studies aiming to develop anti-NRP-1 antibodies as antitumor agents are warranted. Genetech has previously developed monoclonal antibodies for NRP1 with specificity for the CUB (anti-NRP1A) or coagulation factor V/VIII (anti-NRP1B) domains of NRP1, which have been demonstrated to inhibit VEGF-induced cell migration and tumor formation in human umbilical vein endothelial cells and animal models, respectively (40). Anti-NRP1 monoclonal antibodies also block the binding of VEGF to NRP1, thus enabling them to have an additive effect in reducing tumor growth when combined with anti-VEGF therapies (41). Currently in phase-1 development is a human NRP1 antibody, MNRP1685A, which is being investigated individually and in combination with bevacizumab with or without paclitaxel for the treatment of advanced solid tumors (32).

Due to the involvement of NRP-1 in the development of malignant tumors and potential advantages of anti-NRP-1 mAbs as a cancer therapy, studies into novel anti-NRP-1 mAbs with greater specificity are warranted. Previous studies by our group have identified an mAb (A6-26-11-26 clone) against the b1/b2 domains of NRP-1 (abbreviation: anti-NRP-1 mAb) (22,42,43), first discovered by Li *et al* (42), who employed a hybridoma method to screen for b1/b2-specific mAbs. Subsequent analysis by western blotting indicated that the anti-NRP-1 mAb may combine with recombinant human NRP-1-b1/b2 protein fragments and whole NRP-1 proteins expressed by tumor cells (42). Chen *et al* (43) also investigated the effects of the anti-NRP-1 mAb on glioma cell lines *in vitro* and on nude mice bearing glioma tumor *in vivo*, where it was observed that that the anti-NRP-1 mAb inhibited the proliferation, migration and invasion of glioma cells. Furthermore, the anti-NRP-1 mAb may specifically target cancer cells in xenografted glioma tumors and reduce their proliferative properties in nude mice (43). Zeng *et al* (22) recently documented that the anti-NRP-1 mAb inhibited the proliferation and adhesion of human breast cancer MCF7 cells in a dose-dependent manner, while also inhibiting fibronectin-dependent formation of actin stress fibers. In MCF7 cells, the anti-NRP-1 mAb may also inhibit the formation of NRP-1-α5β1 integrin complexes and suppress the phosphorylation of focal adhesion kinase and p130Cas (22). However, in order to implement the anti-NRP-1 mAb in clinical trials, its effects and mechanisms of action in other types of malignant tumors warrant further study. In particular, the effects of the anti-NRP-1 on human gastric cancer remain unknown. Therefore, the present study investigated the effects of the anti-NRP-1 mAb on human gastric cancer cells *in vitro* and *in vivo* and the potential molecular events involved.

Materials and methods

Cell lines. Human gastric cancer cell lines (BGC-823, SGC-7901 and MKN-74) from the Cancer Research Center (CRC) at the Medical College of Xiamen University (Xiamen, China) were preserved in the laboratory prior to experiments.

Western blot analysis. Western blot analysis was performed according to a modified version of previously described methods (27,44,45). Briefly, BGC-823, SGC-7901 and MKN-74 cells were cultured in RPMI-1640 medium (Sigma-Aldrich; Merck KGaA, Darmstadt, Germany) supplemented with 10% heat-inactivated fetal bovine serum (FBS; Gibco; Thermo Fisher Scientific, Inc., Waltham, MA, USA), 100 U/ml penicillin (Sigma-Aldrich; Merck KGaA) and 100 μg/ml streptomycin (Sigma-Aldrich; Merck KGaA) at 37˚C in a humidified atmosphere containing 5% CO_2 for 48 h. Cells were then harvested and lysed for 30 min on ice in lysis buffer [50 mM Tris-hydrogen chloride (pH 7.5), 150 mM sodium chloride (NaCl), 1% nonionic polyoxyethylene-40, 1 mM EDTA, 0.25% sodium deoxycholate, 1 mM sodium fluoride, 1 mM sodium orthovanadate, 5 μg/ml leupeptin, 5 μg/ml aprotinin and 1 mM phenylmethylsulfonyl fluoride], followed by centrifugation at 20,217 x g for 20 min at 4˚C. Protein concentrations of the resulting supernatants (containing whole-cell lysates) were determined with a Bradford protein assay kit (Bio-Rad Laboratories, Inc., Hercules, CA, USA), according to the manufacturer's protocol. Isolated protein samples (5 μg per lane) were then separated using a 10% SDS-PAGE gel before transfer to a polyvinylidene difluoride membrane (EMD Millipore, Billerica, MA, USA). After blocking with 5% (w/v) dried skimmed milk in Tris-buffered saline-Tween-20 (TBST) buffer (50 mM Tris, 150 mM NaCl, 100 mM potassium chloride and 0.1% (v/v) Tween-20 at pH 7.4), membranes were incubated with the following primary antibodies at 4˚C for 12 h: Mouse anti-NRP-1 b1/b2 mAb (1:100; Cancer Research Centre, Medical College of Xiamen University, Xiamen, China), rabbit anti-Akt (Cat no. 4685; 1:1,000), rabbit anti-phosphorylated (p)-Akt (cat no. 13038; 1:1,000), rabbit anti-extracellular signal-regulated kinase (ERK)-1/2 (cat no. 4695; 1:1,000), rabbit anti-p-ERK1/2 (cat no. 4370; 1:2,000), rabbit anti-c-Jun N-terminal kinase (JNK, cat no. 9252, 1:1,000), rabbit anti-p-JNK (cat no. 4668; 1:1,000; all from Cell Signaling Technology, Inc., Danvers, MA, USA), rabbit anti-P38 mitogen-activated protein kinase (P38 MAPK; cat no. ab170099, 1:1,000), rabbit anti-p-P38 (cat no. ab178867; 1:1,000; both from Abcam, Cambridge, UK) and mouse anti-GAPDH (cat no. MA5-15738; 1:2,000; Thermo Fisher Scientific, Inc.). Antibody binding was detected with secondary antibody conjugated to horseradish peroxidase (GE Healthcare Life Sciences, Chalfont, UK) at 37˚C for 1h and bands were visualized using Luminata Forte Western HRP substrate (Merck KGaA), according to the manufacturer's protocol. Immunoreactive signals were quantified using Image J 1.43 software (National Institutes of Health, Bethesda, MD, USA). The level of β-actin protein was used in parallel as a loading

control (cat. no. 4970; 1:1,000; Cell Signaling Technology, Inc.). Based on results of western blotting, BGC-823 cells were used in subsequent analyses.

Reverse transcription-semi-quantitative polymerase chain reaction (RT-semi qPCR). Total RNA was isolated from BGC-823 cells using TRIzol® reagent (Thermo Fisher Scientific, Inc.) and reverse transcribed using random primers in a 20 μl reaction system (RevertAid RT Reverse Transcription kit; Thermo Fisher Scientific, Inc.), according to the manufacturer's protocol. The resulting cDNA templates were amplified by PCR using specific primers for NRP-1 and Taq DNA polymerase (Sangon Biotech Co., Ltd., Shanghai, China). Primer sequences for PCR were as follows (100 mM each): NRP-1 forward, 5'-CACATTGGGCGTTACTGTGGA CA-3' and NRP-1 reverse, 5'-GGAAGTCATCACCTGTTC CACTG-3'. The PCR procedure included pre-denaturation at 95˚C for 5 min, followed by 30 cycles of denaturation at 95˚C for 35 sec, annealing at 57˚C for 45 sec and extension at 72˚C for 80 sec; after finishing the cycles, there was a final-extension at 72˚C for 10 min. Then PCR products were electrophoresed on 1.2% agarose in Tris-borate buffer and visualized using ethidium bromide staining.

Immunofluorescence assay. BGC-823 cells were plated onto glass chamber slides at a density of $1x10^4$ cells/well (Thermo Fisher Scientific, Inc.) and cultured in RPMI-1640 medium at 37˚C in a humidified atmosphere containing 5% CO_2 for 24 h. Following culture, cells were fixed with 4% paraformaldehyde at 37˚C for 30 min and blocked with bovine serum albumin (BSA) at 37˚C for 1 h. Cells were then incubated with anti-NRP-1 mAb (1:100; Cancer Research Centre, Medical College of Xiamen University) for 1 h at 37˚C, followed by anti-mouse IgG tetramethylrhodamine (TRITC)-conjugated secondary antibodies (cat. no. ab6786; 1:1,000; Abcam) for 1 h at 37˚C. After four washes in TBST, cells were stained with Hochest 33258 (Invitrogen; Thermo Fisher Scientific, Inc.) at 37˚C for 10 min and examined using a Zeiss LSM 710 confocal laser scanning microscope (Zeiss GmbH, Jena, Germany). Isotype control antibody of anti-NRP-1 mAb was used as the control (cat. no. ab81032; 1:1,000; Abcam).

Cell viability and viability assay. BGC-823 cells were seeded at a density of $3x10^3$ cells/well in 96-well plates with 100 μl RPMI-1640 medium containing 2% FBS at 37˚C in a humidified atmosphere containing 5% CO_2 for 24 h, then incubated with different concentrations (0, 25, 50, 100, 150, 200 and 400 μg/ml) of anti-NRP-1 mAb (1:100 dilution) at 37˚C for different time periods (24, 48 and 72 h). Cells incubated in the absence of anti-NRP-1 mAb served as a negative control. Following incubation, 20 μl MTT reagent (Sigma-Aldrich; Merck KGaA) in phosphate-buffered saline (PBS) was added into each well and cells were incubated at 37˚C for 4 h, to enable the formation of water insoluble formazan crystals. The formazan crystals were then dissolved in dimethyl sulfoxide (DMSO; 200 μl/well) and their absorbance (optical density, OD) at 570 nm was measured with a microplate spectrophotometer (Bio-Rad Laboratories, Inc.). The inhibition rate of cell viability was calculated using the following equation: Inhibition rate (%)=$(OD_{control}-OD_{treated})/OD_{control}$, as described previously (46,47).

Cell migration and invasion assays. Migration assays were performed in standard 24-well Boyden chambers (Corning, Inc., Corning, NY, USA) according to a modified version of previously described methods (44,48,49). Briefly, $2x10^4$ BGC-823 cells were suspended in 200 μl of RPMI-1640 medium supplemented with 0.1% BSA plus 100 μg/ml anti-NRP-1 mAb before being seeded into the upper chamber, while 500 μl of RPMI-1640 medium supplemented with 10% FBS plus 25 or 100 μg/ml anti-NRP-1 mAb was added to the lower chamber. After 12 h incubation at 37˚C, non-migrated cells on the top side of the Transwell membranes were removed, while migrated cells on the underside of the transwell membranes were fixed with methanol at 37˚C for 20 min and stained with 0.1% crystal violet (Sigma-Aldrich; Merck KGaA) at 37˚C for 5 min. Stained cells from each well were counted in five randomly selected fields at x100 magnification using an eyepiece-indexed graticule (100 grids) and a AE31/CCIS long working distance inverted microscope (Motic, Kowloon, Hong Kong).

Invasion assays were carried out using a similar protocol. Briefly, membrane inserts were coated with Matrigel (BD Biosciences, San Jose, CA, USA) and prehydrated with 1% FBS-supplemented medium for 30 min prior to the addition of the aforementioned cell suspension. Invasion chambers were then incubated at 37˚C for 12 and 24 h and the number of invaded cells was quantified, as above.

Xenograft tumor models. A total of 15 female BALB/c nude mice (6-7 weeks old; mean weight, 20 g) were purchased from the Laboratory Animal Center of Xiamen University and acclimatized for 2 weeks at 26-28˚C in 40-60% humidity with a 10 h light, 14 h dark cycle. All animal procedures were conducted under approved guidelines of the Animal Care and Use Committee of Xiamen University and ethical approval was obtained from the People's Liberation Army 174th Hospital Medical Ethics Review board (Xiamen, China). A total of $2x10^6$ BGC-823 cells were suspended in 200 μl PBS and subcutaneously injected into the right rear flank of each mouse. Mice were observed daily for signs of tumor growth. When tumors reached a volume of ~100 mm^3, mice were randomized into the following three groups (n=5): i) Control (PBS alone); ii) low dose (1 mg/kg anti-NRP-1 mAb in PBS); and iii) high dose (5 mg/kg anti-NRP-1 mAb in PBS). A total of 7 doses of anti-NRP-1 mAb or PBS were administered by intravenous injection into the tail vein every 2 days. All treatments lasted for 15 days and the weight and tumor size of each mouse was measured prior to each administration. Tumor volume (TV) was calculated using the formula: TV (mm^3) = 0.52 x $width^2$ x length, as described previously (50). All mice were sacrificed by cervical dislocation under light anesthetic ether 2 days after the last administration and the tumor tissue was immediately isolated in order to measure the wet weight of xenografted tumor tissue.

Immunohistochemical analysis. Immunohistochemical analysis was performed according to a modified version of a previously described method (44). Briefly, tumors tissues were frozen in optimal cutting temperature compound for 1 h and 5-μm sections were cut and mounted onto glass slides. Slides were then fixed with 10% neutral-buffered formalin at

37˚C for 1 h and washed with PBS. Slides were subsequently stained with hematoxylin and eosin, blocked with 5% sheep serum (Beyotime Institute of Biotechnology, Haimen, China) for 30 min at 37˚C and incubated with rabbit anti-VEGF antibody (cat no. ab52917; 1:100; Abcam) at 4˚C for 12 h. Following counterstaining with Gill No. 3 hematoxylin solution (Sigma-Aldrich; Merck KGaA) at 37˚C for 1 min, sections were dehydrated in a descending ethanol series, cleared with xylene and mounted for viewing. Immunostained VEGF was quantified using Image-Pro® Plus 6.0 software (Media Cybernetics, Inc., Rockville, MD, USA). Integrated OD (IOD), as a quantitative measure of staining intensity, was calculated to determine the level of protein expression, as described previously (51,52).

Statistical analysis. For all *in vitro* experiments, data are presented as the mean ± standard deviation of at least three independent experiments. Statistical analysis was performed with SPSS 18.0 software (SPSS, Inc., Chicago, IL, USA). Differences among groups were analyzed by one way analysis of variance with a Tukey's multiple comparisons test and $P<0.05$ was considered to indicate a statistically significant difference.

Results

NRP-1 is expressed in human gastric cancer cells. The expression of NRP-1 protein in human gastric cancer cell lines (BGC-823, SGC-7901 and MKN-74) was evaluated using western blot analysis. It was observed that all the gastric cancer cell lines constitutively express NRP-1, with BGC-823 cells expressing relatively high levels of NRP-1 (Fig. 1A). For BGC-823 cells, the expression of NRP-1 was subsequently verified by RT-PCR (Fig. 1B). Furthermore, an immunofluorescence assay was performed to identify the distribution of NRP-1 in BGC-823 cells, using anti-NRP-1 mAb as the primary antibody, with results indicating that NRP-1 protein is predominantly distributed in the cytomembrane and cytoplasm regions of BGC-823 cells (Fig. 1C).

Anti-NRP-1 mAb has little effect on the survival and viability of human gastric cancer BGC-823 cells. The effects of anti-NRP-1 mAb on the survival and viability of BGC-823 cells were determined by an MTT assay (Fig. 2). When BGC-823 cells were treated with lower concentrations of anti-NRP-1 mAb (25 to 150 μg/ml) for different time periods (24, 48 and 72 h), it was observed that anti-NRP-1 mAb had a minor effect on the viability of BGC-823 cells (average inhibition, 1.53-6.21%), though the inhibitory effects of anti-NRP-1 did not significantly differ ($P>0.05$). By contrast, at higher concentrations of anti-NRP-1 mAb (200 and 400 μg/ml), the viability of BGC-823 cells was significantly inhibited (average inhibition, 12.83-27.52%; $P<0.05$). However, due to the high concentration of anti-NRP-1 mAb required to inhibit cellular viability (>150 μg/ml), these results indicate that anti-NRP-1 mAb (<150 μg/ml) has little to no effect on BGC-823 cell viability.

Anti-NRP-1 mAb suppresses the migration and invasion of BGC-823 cells. Lower concentrations of anti-NRP-1 mAb did not significantly affect the viability of BGC-823 cells. Therefore, the influence of anti-NRP-1 mAb on the migration and invasion of BGC-823 cells was subsequently evaluated. In a Transwell migration assay (Fig. 3A), BGC-823 cells treated with 25 and 100 μg/ml anti-NRP-1 mAb for 12 h exhibited significant decreases in migratory ability, relative to control cells (23.31 and 42.89% decreases, respectively; both $P<0.05$; Fig. 3B). In addition, in a 12-h Matrigel assay (Fig. 3C), the 25 and 100 μg/ml anti-NRP-1 mAb groups exhibited significant decreases in their invasive abilities, relative to control cells (both $P<0.01$; Fig. 3D). This effect was also observed after 24 h (Fig. 3E), whereby low and high dose BGC-823 cells exhibited significant decreases in their invasive abilities, relative to control cells (15.07 and 23.10% decreases, respectively; both $P<0.05$; Fig. 3F). Collectively these data indicate that anti-NRP-1 mAb may suppress the migration and invasion of human gastric cancer BGC-823 cells.

Anti-NRP-1 mAb inhibits Akt phosphorylation in BGC-823 cells. To determine whether the effects of anti-NRP-1 mAb on BGC-823 cell migration and invasion were through the phosphoinositide 3-kinase (PI3K)/Akt and MAPK signaling pathways, the phosphorylation levels of key signaling molecules (Akt, ERK, p38 and JNK) were measured following treatment with anti-NRP-1 mAb. Data from a western blot analysis indicated that the levels of p-Akt were markedly reduced following anti-NRP-1 mAb treatment at 25 and 100 μg/ml (Fig. 4A and B) doses. Specifically, reductions in p-Akt were observed in the anti-NRP-1 mAb treatment groups (25 and 100 μg/ml) at the first time point measured (10 min) and p-Akt was difficult to detect at later time points (30 and 60 min). However, no obvious changes to the phosphorylation levels of MAPK signaling molecules (ERK, p38 and JNK) were observed following low and high dose anti-NRP-1 mAb treatment (Fig. 4A and B).

Anti-NRP-1 mAb inhibits the growth of human gastric cancer xenografts. Data on the growth characteristics of subcutaneous xenograft tumors (Fig. 5A and B) indicated that anti-NRP-1 mAb suppressed the growth of xenograft tumors in nude mice. Following seven administrations of 1 and 5 mg/kg anti-NRP-1 mAb over 15 days, the final volumes of xenograft tumors were reduced by 34.93 and 56.85%, respectively (Fig. 5A). In detail, for 5 mg/kg antibody, tumor volume was significantly reduced on days 9, 11, 13 (all $P<0.05$) and 15 ($P<0.01$), while 1 mg/ml antibody induced significant reduction in tumor volume on day 15 ($P<0.05$), relative to untreated controls. Similarly, treatment with 1 and 5 mg/kg anti-NRP-1 mAb decreased final tumor weights by 24.16 and 63.09% respectively; an effect deemed to be significant for 5 mg/kg anti-NRP-1 mAb, relative to untreated controls ($P<0.01$; Fig. 5B). In addition, toxicity-dependent weight loss was not observed in tumor-bearing mice treated with anti-NRP-1 mAb (Fig. 5C).

Anti-NRP-1 mAb downregulates VEGF protein expression in human gastric cancer xenografts. As anti-NRP-1 mAb suppressed the growth of xenograft tumors in nude mice, the potential underlying molecular events were subsequently evaluated, by measuring the level of VEGF expression in gastric cancer xenografts. Data from immunohistochemical

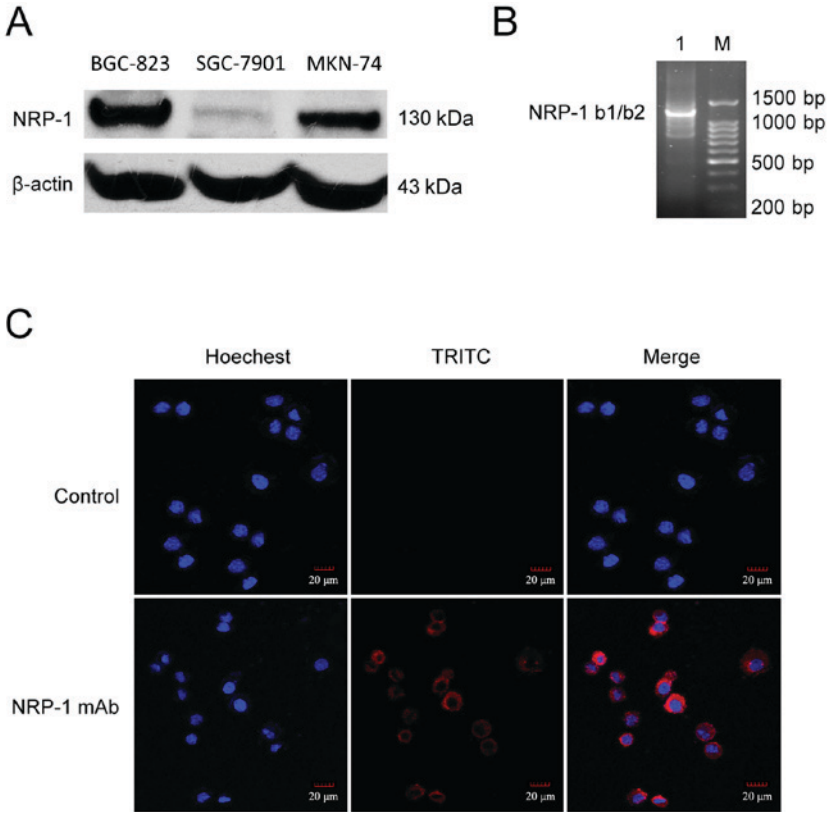

Figure 1. Expression and distribution of NRP-1 in human gastric cancer cells. (A) Levels of NRP-1 protein expression in human gastric cancer cell lines (BGC-823, SGC-7901 and MKN-74) measured by western blot analysis. β-actin was used as an internal control. (B) Levels of NRP-1 mRNA in BGC-823 cells measured by reverse transcription-quantitative polymerase chain reaction. (C) The distribution of NRP-1 proteins in BGC-823 cells measured by confocal fluorescence microscopy. Hoechst staining (blue) indicates cell nuclei and TRITC staining (red) indicates NRP-1 expression. Magnification, x400. Scale bar, 20 μm. NRP-1, neuropilin 1; b1/b2, coagulation factor V/VIII homology-like domains; mAb, monoclonal antibody; BGC-823, SGC-7901 and MKN-74, human gastric cancer cell lines; TRITC, tetramethylrhodamine.

analysis (Fig. 6) demonstrated that the IOD of VEGF was significantly decreased in the anti-NRP-1 mAb treatment groups (1 and 5 mg/kg), relative to the negative control group (P<0.01; Fig. 6B). In turn, reduction in the IOD of VEGF was significantly greater in the 5 mg/kg anti-NRP-1 mAb treatment group, relative to that in the 1 mg/kg anti-NRP-1 mAb group (P<0.01; Fig. 6B). These data indicate that VEGF expression may be downregulated by anti-NRP-1 mAb in a dose-dependent manner.

Discussion

Preclinical data indicate that NRP-1 may have roles in tumor cell proliferation and pathological angiogenesis, thus making it a potential anticancer target (23,41). However, for patients to clinically benefit from anti-NRP-1 therapies, it may be necessary to first determine the expression patterns of NRP-1. Numerous studies have reported *in situ* expression patterns of NRP-1 in human tissues, including gastric (18), prostate (20), pancreatic (53), colorectal (15), breast (16,54) and lung cancer (17,55). Therefore, the present study measured the expression of NRP-1 in human gastric cancer cell lines (BGC-823, SGC-7901 and MKN-74). Results demonstrated that all three cell lines constitutively expressed NRP-1 at the mRNA and protein level, with BGC-823 cells expressing relatively higher levels of NRP-1. These data are consistent with a previous study by Akagi *et al* (56), whereby the expression

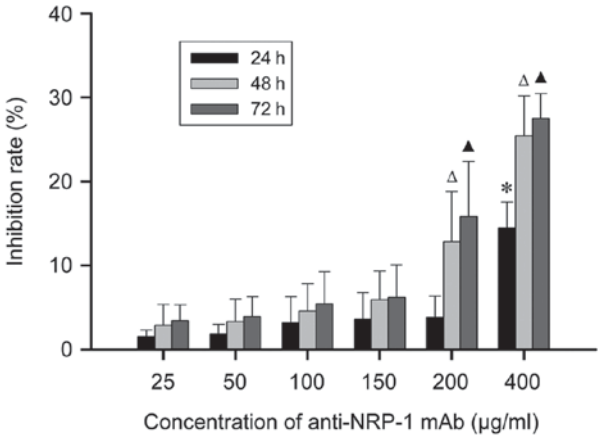

Figure 2. Effect of anti-NRP-1 mAb on BGC-823 cell viability. BGC-823 cells were administered with different concentrations (25-400 μg/ml) of anti-NRP-1 mAb for 24, 48 and 72 h, respectively. The viability and viability rates of cells were subsequently measured by an MTT assay. Data are expressed as mean ± standard deviation of four independent experiments. *P<0.01 vs. 25-200 μg/ml anti-NRP-1 mAb groups at 24 h, $^{\Delta}$P<0.05 vs. all other anti-NRP-1 mAb treatment groups at 48 h, $^{\blacktriangle}$P<0.01 vs. all other anti-NRP-1 mAb treatment groups at 72 h. NRP-1, neuropilin 1; mAb, monoclonal antibody; BGC-823, human gastric cancer cell line.

of NRP-1 was detected in five of seven human gastric cancer cell lines (TMK-1, AGS, NCI-N87, ST-2 and ST-7). It was additionally observed in the current study that NRP-1 protein

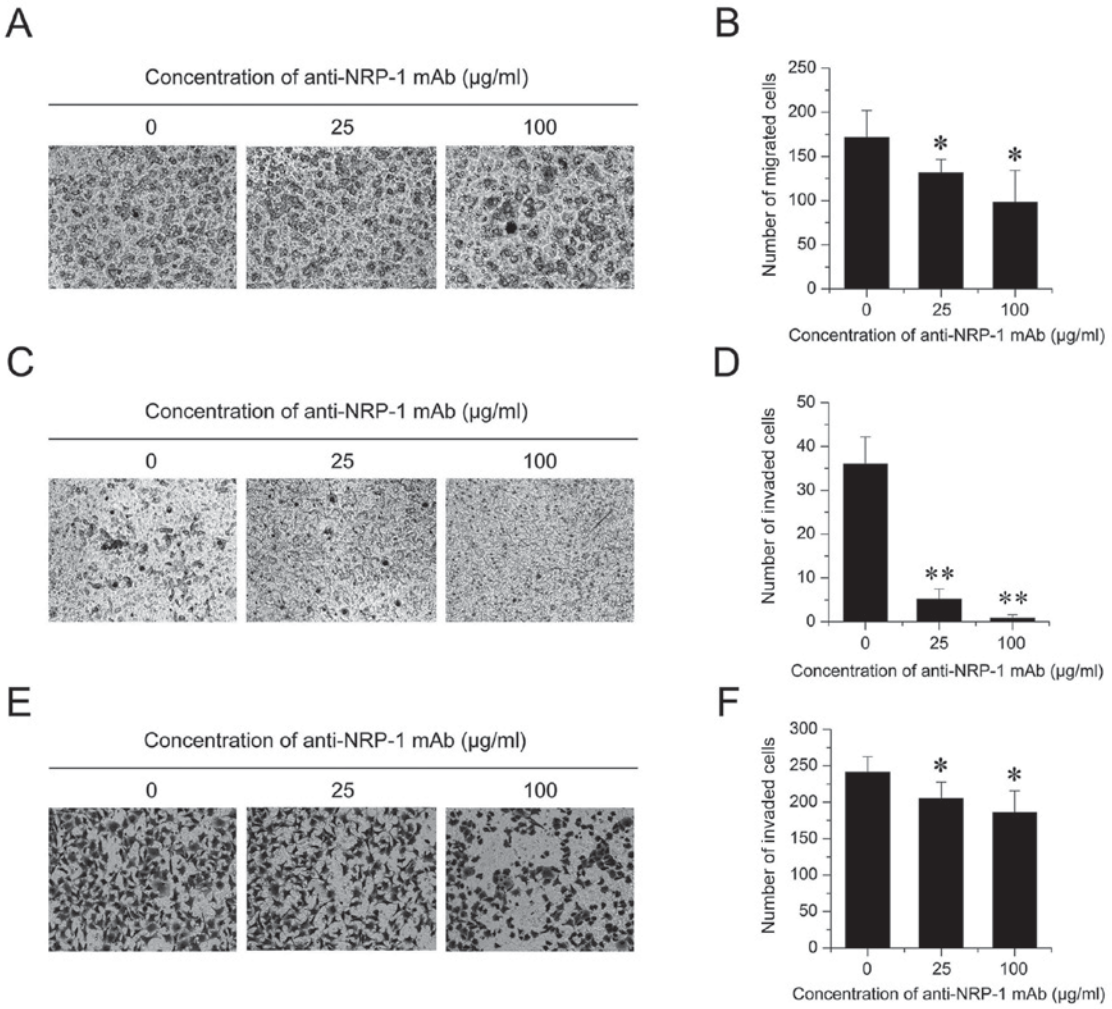

Figure 3. Anti-NRP-1 mAb suppresses BGC-823 cell migration and invasion. (A and B) A Transwell migration assay was performed to determine the migratory rate of BGC-823 cells treated with different concentrations of anti-NRP-1 mAb (0, 25 and 100 μg/ml) for 12 h. (A) Representative images of migrated cells stained with crystal violet are shown (magnification, x100). (B) Quantification of migrated cells. (C-F) A Transwell invasion assay was also performed on BGC-823 cells treated with anti-NRP-1 mAb-treated (0, 25 and 100 μg/ml). (C) Representative images of invaded cells across a Matrigel-coated membrane following 12 h treatment with anti-NRP-1 mAb are shown (magnification, x100). (D) Quantification of invaded cells following 12 h anti-NRP-1 mAb treatment. (E) Representative images of invaded cells following 24 h treatment with anti-NRP-1 mAb are shown (magnification, x100). (F) Quantification of invaded cells following 24 h anti-NRP-1 mAb treatment. All data are presented as the mean ± standard deviation of three independent experiments. *P<0.05 and **P<0.01 vs. control cells. NRP-1, neuropilin 1; mAb, monoclonal antibody; BGC-823, human gastric cancer cell line; control, untreated BGC-823 cells.

was predominantly distributed in the cytomembrane and cytoplasm of BGC-823 cells.

In a previous study by our group, the anti-NRP-1 mAb (6.25-100 μg/ml) was demonstrated to inhibit the growth and proliferation of human glioma cell lines (U251 and U87) and a rat glioma cell line (C6) in a concentration- and time-dependent manner. For instance, at a dose of 100 μg/ml anti-NRP-1 mAb, U251 cell growth was inhibited by 76.26% (43). Zeng *et al* (22) also demonstrated that the anti-NRP-1 mAb (200 and 400 μg/ml) significantly inhibited the proliferation of MCF7 human breast cancer cells, observed as significant reductions in the number and size of MCF7 cell colonies 7 days after mAb administration. However, 25-100 μg/ml anti-NRP-1 mAb had little to no effect on MCF7 cell growth and proliferation. Similarly, the current study demonstrated that treatment with <150 μg/ml anti-NRP-1 mAb had little to no effect on BGC-823 cell viability, while 200 or 400 μg/ml doses of anti-NRP-1 mAb were able to significantly inhibit BGC-823 cell viability.

High-affinity mAbs that target the CUB domains (anti-NRP-1A) or coagulation factors V/VIII domains (anti-NRP-1B) of NRP-1 have been previously developed by Genetech, though it was demonstrated that anti-NRP-1 mAb alone (anti-NRP-1A or -1B) or in combination with anti-VEGF did not alter the proliferation of a human NSCLC cell line SK-MES-1 *in vitro*. In addition, both anti-NRP1 mAbs were unable to induce cytotoxicity in human ductal carcinoma (BT-474) or SK-MES-1 cell lines (40). It has also been demonstrated that anti-NRP-1A mAb had no effect on VEGF-induced endothelial cell (EC) proliferation and anti-NRP-1B mAb only stimulated a slight dose-responsive reduction, thus indicating that the inhibitory effects of anti-NRP1 mAb on SK-MES-1 tumor growth are not through the alteration of tumor blood vessels (41). Furthermore, knockdown of NRP-1 in ECs by small interfering RNA only partially inhibited VEGF-induced proliferation, suggesting that the primary role of NRP-1 in VEGF-driven EC behavior is to mediate cell migration (57).

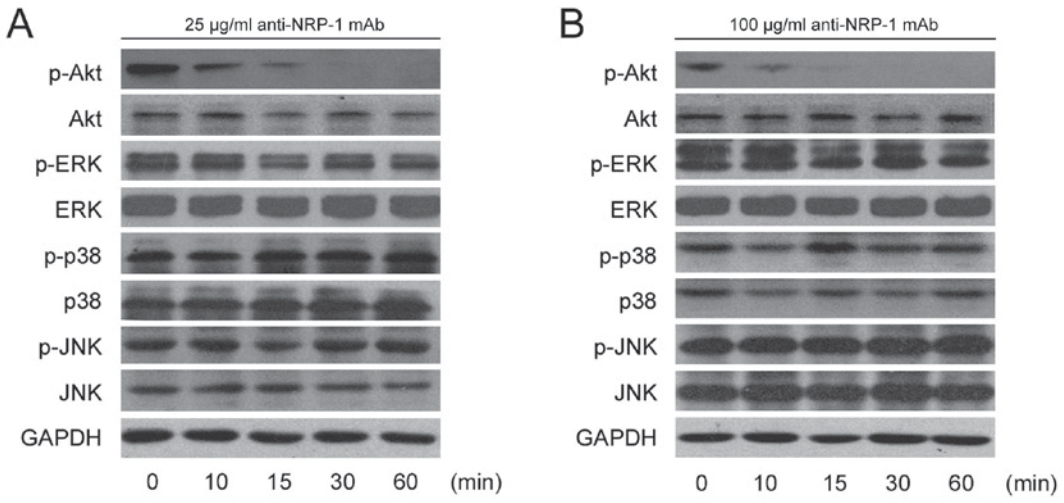

Figure 4. Anti-NRP-1 mAb downregulates p-Akt in human gastric cancer BGC-823 cells. Serum-starved BGC-823 cells were incubated with (A) 25 μg/ml anti-NRP-1 mAb or (B) 100 μg/ml anti-NRP-1 mAb for the indicated time periods. Cellular proteins were extracted and 50 μg whole-cell protein extracts were subjected to western blot analysis using primary antibodies against p-Akt, Akt, p-ERK, ERK, p-JNK, JNK, p-P38, P38 and GAPDH. GAPDH was used as a loading control. Representative immunoblots from three independent experiments are shown. NRP-1, neuropilin 1; mAb, monoclonal antibody; BGC-823, human gastric cancer cell line; p-, phosphorylated; ERK, extracellular signal-regulated protein kinase; JNK, c-Jun N-terminal kinase; P38, P38 mitogen- activated protein kinase.

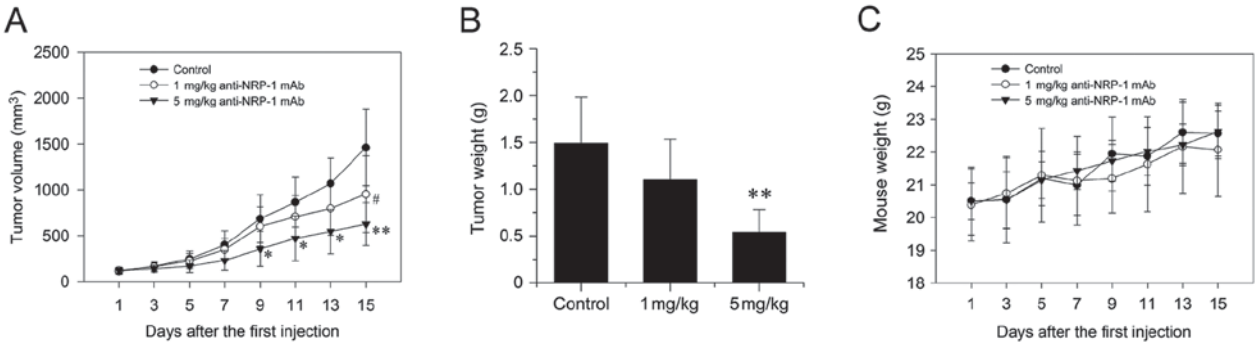

Figure 5. Anti-NRP-1 mAb inhibits the growth of human gastric cancer xenograft in nude mice. (A) Xenograft tumor volume over the 15 d treatment period. *P<0.05, **P<0.01 and $^{\#}$P<0.05 vs. control. (B) Wet weights of xenograft tumors on day 15 of the treatment period **P<0.01 vs. control. (C) Weights of tumor-bearing mice treated with anti-NRP-1 mAb. The weights of mice in all three groups did not significantly differ during the treatment period, indicating a lack of toxicity-dependent weight loss. Data are expressed as the mean ± standard deviation (n=5). NRP-1, neuropilin 1; mAb, monoclonal antibody; control, phosphate-buffered saline-treated tumor-bearing mice.

As anti-NRP-1 mAb exhibited no significant effect on BGC-823 cell viability, the current study evaluated whether anti-NRP-1 mAb regulated the migration and invasion of BGC-823 cells. Results of a standard Boyden chamber assay indicated that anti-NRP-1 mAb may suppress BGC-823 cell migration and invasion. In a previous study by our group, the migration and invasion of human glioma U251 and U87 cells and rat glioma C6 cells were inhibited after treatment with anti-NRP-1 mAb (43). Similarly, Pan *et al* (41) documented that treatment with anti-NRP-1A and anti-NRP-1B significantly reduced EC migration, with anti-NRP-1B exhibiting stronger inhibitory effects. Ochiumi *et al* (8) also demonstrated that cell migration was decreased following knockdown of NRP-1 in WiDR cells (human colon adenocarcinoma cell line) by RNA interference.

The PI3K/Akt and MAPK signaling pathways are involved in a range of cellular functions, including cell survival, growth, proliferation, migration and invasion (58-60). As anti-NRP-1 mAb suppressed BGC-823 cell migration and invasion, the current study investigated the potential molecular events involved. The phosphorylation levels of key signaling molecules (Akt, ERK, p38 and JNK) were measured following anti-NRP-1 mAb treatment. It was observed that the anti-NRP-1 mAb inhibited the phosphorylation of Akt in BGC-823 cells, though anti-NRP-1 mAb treatment did not affect activation of MAPK signaling.

Results of the current study also indicated that anti-NRP-1 mAb may suppress the growth of human gastric cancer xenograft in nude mice *in vivo*. In addition, anti-NRP-1 mAb treatment did not cause toxicity-dependent in tumor-bearing mice. Consistent with present results, our previous study demonstrated that the anti-NRP-1 mAb specifically targeted tumor cells in U87 xenografts, by reducing xenograft proliferation and growth rate (43). Similarly, Pan *et al* (41) used an NSCLC-SK-MES-1 xenograft model, specifically with high expression of NRP-1 in the vascular and stromal tissue

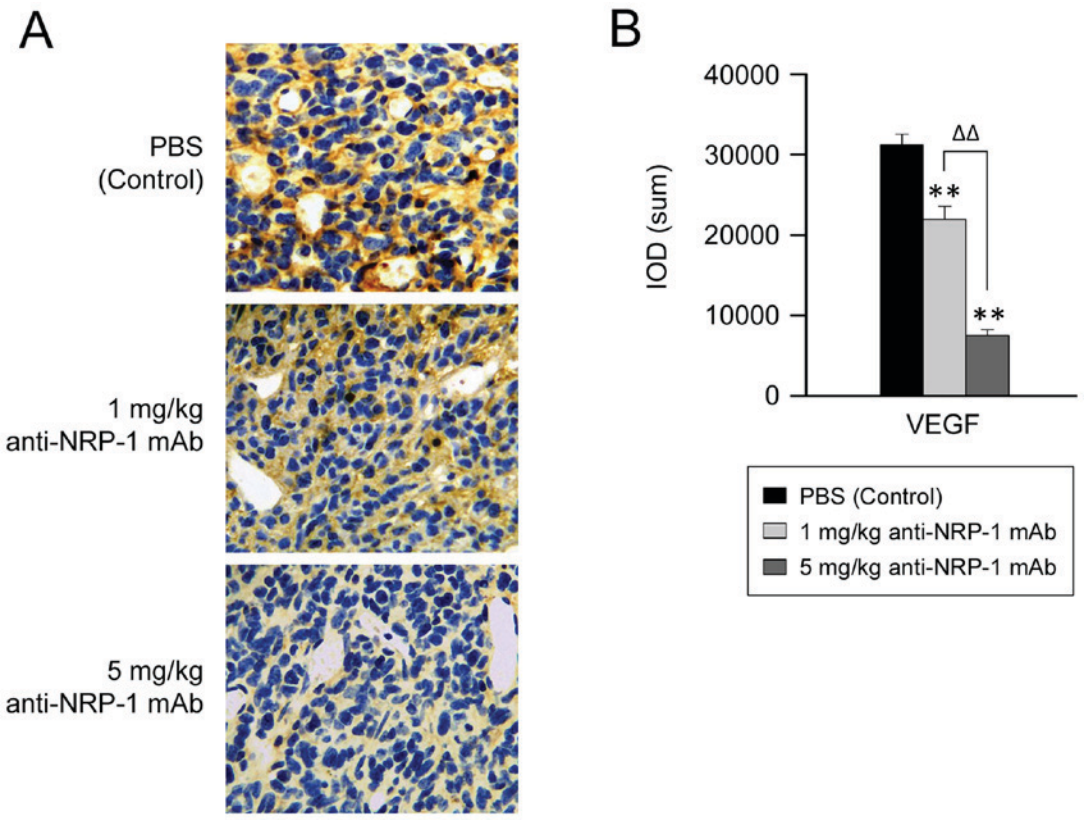

Figure 6. Anti-NRP-1 mAb downregulates the expression of VEGF in human gastric cancer xenograft. (A) Representative immunostaining images of VEGF protein expression are shown (brown, magnification x400). (B) IODs were calculated using Image-Pro® Plus 6.0 software. Bars represent the mean ± standard deviation of three independent experiments (n=5). **P<0.01 vs. control, $^{\Delta\Delta}$P<0.01 vs. 5 mg/kg anti-NRP-1 mAb group. NRP-1, neuropilin 1; mAb, monoclonal antibody; VEGF, vascular endothelial growth factor; IOD, integrated optical density; PBS, phosphate-buffered saline; control, PBS-treated tumor-bearing mice.

and intermediate expression in tumor cells, to determine the effects of NRP-1 blockade on tumor growth inhibition (TGI), initially provided by a VEGF blockade. In this model, individual treatment with anti-VEGF mAb and anti-NRP-1B mAb caused 52 and 37% TGI, respectively, while anti-NRP-1A mAb had no significant effect on TGI. Ochiumi *et al* (8) has documented that cell proliferation was not influenced by the inhibition of NRP-1 expression in WiDR cells *in vitro*. However, it was observed *in vivo* that the proliferation index of cells was significantly greater in tissues exhibiting high levels of NRP-1 staining (8). The reasons for these inconsistencies remain unknown, though it is possible that juxtacrine signaling occurs, whereby VEGF bound to NRP-1 on tumor cells also binds to VEGFR-2 on adjacent ECs, leading to the induction of tumor growth (8,15,61). The current study observed that anti-NRP-1 mAb significantly downregulated VEGF expression in human gastric cancer xenografts, and Xia *et al* (62) previously documented that Akt1 is a key downstream regulator of tumor growth, angiogenesis and VEGF expression. In addition, recent studies have demonstrated that PI3K/Akt signaling regulates the expression of hypoxia-inducible factor (HIF)-1α and VEGF in a number of cancer cell types, including prostate, ovarian, and pancreatic cancer cells, potentially by a cascade effect, whereby activated Akt promotes HIF-1α upregulation, with HIF-1α then inducing the transcriptional activation of VEGF (63-66). Collectively, these results suggest that anti-NRP-1 mAb may inhibit the activation of Akt, thus decreasing HIF-1 and VEGF expression and inhibiting gastric cancer xenograft growth *in vivo*.

In conclusion, the present study demonstrated that the migration and invasion of gastric cancer BGC-823 cells was suppressed by treatment with anti-NRP-1 mAb *in vitro*. By contrast, anti-NRP-1 mAb had little effect on BGC-823 cell viability. While the underlying mechanisms regarding the effects of anti-NRP-1 mAb remain unknown, it was observed that treatment with anti-NRP-1 mAb inhibited the phosphorylation of Akt in BGC-823 cells. It was also demonstrated *in vivo* that anti-NRP-1 mAb downregulated the expression of VEGF and suppressed the growth of gastric cancer xenografts in mice. These results are consistent with those of previous studies into the effects of anti-NRP-1 mAb on different malignant tumors, thus indicating that NRP-1 inhibition with anti-NRP-1 mAb may have therapeutic effects in the treatment of cancer.

Acknowledgements

Not applicable.

Funding

The current study was supported by the National Natural Science Foundation of China (grant no. 81172970), the Science and Technology Innovative Foundation of Xiamen (grant nos. 3502Z20134026 and 3502Z20144034) and the Medical

Science and Technology Innovation Fund of the Nanjing Military Region of the People's Liberation Army (grant no. 14ZD33).

Availability of data and materials

The datasets used and/or analyzed during the current study are available from the corresponding author on reasonable request.

Authors' contributions

YQC and JHY designed the study, supervised the experiments, reviewed the manuscript and approved the final version to be published. YD performed the experiments, analyzed and interpreted the data and drafted and revised the manuscript. JZ participated in the design of the study, helped perform the experiments and analyzed and interpreted the data. SYW instructed in cellular and molecular techniques; YL, YJM, SHG and YX supplied critical reagents, performed the experiments and participated in the acquisition of data. All authors have read and approved the final version of the manuscript.

Ethics approval and consent to participate

All animal procedures were conducted under approved guidelines of the Animal Care and Use Committee of Xiamen University and ethical approval was obtained from the People's Liberation Army 174th Hospital Medical Ethics Review board.

Consent for publication

Not applicable.

Competing interests

The authors declare that they have no competing interests.

References

1. Fujisawa H, Takagi S and Hirata T: Growth-associated expression of a membrane protein, neuropilin, in Xenopus optic nerve fibers. Dev Neurosci 17: 343-349, 1995.
2. Fujisawa H and Kitsukawa T: Receptors for collapsin/semaphorins. Curr Opin Neurobiol 8: 587-592, 1998.
3. Soker S: Neuropilin in the midst of cell migration and retraction. Int J Biochem Cell Biol 33: 433-437, 2001.
4. He Z and Tessier-Lavigne M: Neuropilin is a receptor for the axonal chemorepellent Semaphorin III. Cell 90: 739-751, 1997.
5. Gray MJ, Wey JS, Belcheva A, McCarty MF, Trevino JG, Evans DB, Ellis LM and Gallick GE: Neuropilin-1 suppresses tumorigenic properties in a human pancreatic adenocarcinoma cell line lacking neuropilin-1 coreceptors. Cancer Res 65: 3664-3670, 2005.
6. Nakamura F, Tanaka M, Takahashi T, Kalb RG and Strittmatter SM: Neuropilin-1 extracellular domains mediate semaphorin D/III-induced growth cone collapse. Neuron 21: 1093-1100, 1998.
7. Pellet-Many C, Frankel P, Jia H and Zachary I: Neuropilins: Structure, function and role in disease. Biochem J 411: 211-226, 2008.
8. Ochiumi T, Kitadai Y, Tanaka S, Akagi M, Yoshihara M and Chayama K: Neuropilin-1 is involved in regulation of apoptosis and migration of human colon cancer. Int J Oncol 29: 105-116, 2006.
9. Chaudhary B, Khaled YS, Ammori BJ and Elkord E: Neuropilin 1: Function and therapeutic potential in cancer. Cancer Immunol Immunother 63: 81-99, 2014.
10. Dzionek A, Fuchs A, Schmidt P, Cremer S, Zysk M, Miltenyi S, Buck DW and Schmitz J: BDCA-2, BDCA-3, and BDCA-4: Three markers for distinct subsets of dendritic cells in human peripheral blood. J Immunol 165: 6037-6046, 2000.
11. Romeo PH, Lemarchandel V and Tordjman R: Neuropilin-1 in the immune system. Adv Exp Med Biol 515: 49-54, 2002.
12. Tordjman R, Lepelletier Y, Lemarchandel V, Cambot M, Gaulard P, Hermine O and Roméo PH: A neuronal receptor, neuropilin-I, is essential for the initiation of the primary immune response. Nat Immunol 3: 477-482, 2002.
13. Herzog Y, Kalcheim C, Kahane N, Reshef R and Neufeld G: Differential expression of neuropilin-1 and neuropilin-2 in arteries and veins. Mech Dev 109: 115-119, 2001.
14. Battaglia A, Buzzonetti A, Monego G, Peri L, Ferrandina G, Fanfani F, Scambia G and Fattorossi A: Neuropilin-1 expression identifies a subset of regulatory T cells in human lymph nodes that is modulated by preoperative chemoradiation therapy in cervical cancer. Immunology 123: 129-138, 2008.
15. Parikh AA, Fan F, Liu WB, Ahmad SA, Stoeltzing O, Reinmuth N, Bielenberg D, Bucana CD, Klagsbrun M and Ellis LM: Neuropilin-1 in human colon cancer: Expression, regulation, and role in induction of angiogenesis. Am J Pathol 164: 2139-2151, 2004.
16. Ghosh S, Sullivan CA, Zerkowski MP, Molinaro AM, Rimm DL, Camp RL and Chung GG: High levels of vascular endothelial growth factor and its receptors (VEGFR-1, VEGFR-2, neuropilin-1) are associated with worse outcome in breast cancer. Hum Pathol 39: 1835-1843, 2008.
17. Hong TM, Chen YL, Wu YY, Yuan A, Chao YC, Chung YC, Wu MH, Yang SC, Pan SH, Shih JY, *et al*: Targeting neuropilin 1 as an antitumor strategy in lung cancer. Clin Cancer Res 13: 4759-4768, 2007.
18. Hansel DE, Wilentz RE, Yeo CJ, Schulick RD, Montgomery E and Maitra A: Expression of neuropilin-1 in high-grade dysplasia, invasive cancer, and metastases of the human gastrointestinal tract. Am J Surg Pathol 28: 347-356, 2004.
19. Evans IM, Yamaji M, Britton G, Pellet-Many C, Lockie C, Zachary IC and Frankel P: Neuropilin-1 signaling through p130Cas tyrosine phosphorylation is essential for growth factor-dependent migration of glioma and endothelial cells. Mol Cell Biol 31: 1174-1185, 2011.
20. Latil A, Bièche I, Pesche S, Valèri A, Fournier G, Cussenot O and Lidereau R: VEGF overexpression in clinically localized prostate tumors and neuropilin-1 overexpression in metastatic forms. Int J Cancer 89: 167-171, 2000.
21. Prud'homme GJ and Glinka Y: Neuropilins are multifunctional coreceptors involved in tumor initiation, growth, metastasis and immunity. Oncotarget 3: 921-939, 2012.
22. Zeng F, Luo F, Lv S, Zhang H, Cao C, Chen X, Wang S, Li Z, Wang X, Dou X, *et al*: A monoclonal antibody targeting neuropilin-1 inhibits adhesion of MCF7 breast cancer cells to fibronectin by suppressing the FAK/p130cas signaling pathway. Anticancer Drugs 25: 663-672, 2014.
23. Jubb AM, Strickland LA, Liu SD, Mak J, Schmidt M and Koeppen H: Neuropilin-1 expression in cancer and development. J Pathol 226: 50-60, 2012.
24. Bergé M, Bonnin P, Sulpice E, Vilar J, Allanic D, Silvestre JS, Lévy BI, Tucker GC, Tobelem G and Merkulova-Rainon T: Small interfering RNAs induce target-independent inhibition of tumor growth and vasculature remodeling in a mouse model of hepatocellular carcinoma. Am J Pathol 177: 3192-3201, 2010.
25. Raskopf E, Vogt A, Standop J, Sauerbruch T and Schmitz V: Inhibition of neuropilin-1 by RNA-interference and its angiostatic potential in the treatment of hepatocellular carcinoma. Z Gastroenterol 48: 21-27, 2010.
26. Lu L, Zhang L, Xiao Z, Lu S, Yang R and Han ZC: Neuropilin-1 in acute myeloid leukemia: Expression and role in proliferation and migration of leukemia cells. Leuk Lymphoma 49: 331-338, 2008.
27. Barr MP, Byrne AM, Duffy AM, Condron CM, Devocelle M, Harriott P, Bouchier-Hayes DJ and Harmey JH: A peptide corresponding to the neuropilin-1-binding site on VEGF(165) induces apoptosis of neuropilin-1-expressing breast tumour cells. Br J Cancer 92: 328-333, 2005.
28. Tirand L, Frochot C, Vanderesse R, Thomas N, Trinquet E, Pinel S, Viriot ML, Guillemin F and Barberi-Heyob M: A peptide competing with VEGF165 binding on neuropilin-1 mediates targeting of a chlorin-type photosensitizer and potentiates its photodynamic activity in human endothelial cells. J Control Release 111: 153-164, 2006.

29. Jia H, Cheng L, Tickner M, Bagherzadeh A, Selwood D and Zachary I: Neuropilin-1 antagonism in human carcinoma cells inhibits migration and enhances chemosensitivity. Br J Cancer 102: 541-552, 2010.
30. Jarvis A, Allerston CK, Jia H, Herzog B, Garza-Garcia A, Winfield N, Ellard K, Aqil R, Lynch R, Chapman C, *et al*: Small molecule inhibitors of the neuropilin-1 vascular endothelial growth factor A (VEGF-A) interaction. J Med Chem 53: 2215-2226, 2010.
31. Gagnon ML, Bielenberg DR, Gechtman Z, Miao HQ, Takashima S, Soker S and Klagsbrun M: Identification of a natural soluble neuropilin-1 that binds vascular endothelial growth factor: In vivo expression and antitumor activity. Proc Natl Acad Sci USA 97: 2573-2578, 2000.
32. Grandclement C and Borg C: Neuropilins: A new target for cancer therapy. Cancers (Basel) 3: 1899-1928, 2011.
33. Starzec A, Ladam P, Vassy R, Badache S, Bouchemal N, Navaza A, du Penhoat CH and Perret GY: Structure-function analysis of the antiangiogenic ATWLPPR peptide inhibiting VEGF(165) binding to neuropilin-1 and molecular dynamics simulations of the ATWLPPR/neuropilin-1 complex. Peptides 28: 2397-2402, 2007.
34. Bondeva T, Rüster C, Franke S, Hammerschmid E, Klagsbrun M, Cohen CD and Wolf G: Advanced glycation end-products suppress neuropilin-1 expression in podocytes. Kidney Int 75: 605-616, 2009.
35. Bondeva T and Wolf G: Advanced glycation end products suppress neuropilin-1 expression in podocytes by a reduction in Sp1-dependent transcriptional activity. Am J Nephrol 30: 336-345, 2009.
36. Bondeva T, Wojciech S and Wolf G: Advanced glycation end products inhibit adhesion ability of differentiated podocytes in a neuropilin-1-dependent manner. Am J Physiol Renal Physiol 301: F852-F870, 2011.
37. Teesalu T, Sugahara KN, Kotamraju VR and Ruoslahti E: C-end rule peptides mediate neuropilin-1-dependent cell, vascular, and tissue penetration. Proc Natl Acad Sci USA 106: 16157-16162, 2009.
38. Haspel N, Zanuy D, Nussinov R, Teesalu T, Ruoslahti E and Aleman C: Binding of a C-end rule peptide to the neuropilin-1 receptor: A molecular modeling approach. Biochemistry 50: 1755-1762, 2011.
39. Rizzolio S, Rabinowicz N, Rainero E, Lanzetti L, Serini G, Norman JC, Neufeld G and Tamagnone L: Neuropilin-1 dependent regulation of EGF-Receptor signaling. Cancer Res 72: 5801-5811, 2012.
40. Liang WC, Dennis MS, Stawicki S, Chanthery Y, Pan Q, Chen Y, Eigenbrot C, Yin J, Koch AW, Wu X, *et al*: Function blocking antibodies to neuropilin-1 generated from a designed human synthetic antibody phage library. J Mol Biol 366: 815-829, 2007.
41. Pan Q, Chanthery Y, Liang WC, Stawicki S, Mak J, Rathore N, Tong RK, Kowalski J, Yee SF, Pacheco G, *et al*: Blocking neuropilin-1 function has an additive effect with anti-VEGF to inhibit tumor growth. Cancer Cell 11: 53-67, 2007.
42. Li X, Luo F, Wang S, Ni E, Tang X, Lv H, Chen X, Chen L and Yan J: Monoclonal Antibody Against NRP-1 b1b2. Hybridoma (Larchmt) 30: 369-373, 2011.
43. Chen L, Miao W, Tang X, Zhang H, Wang S, Luo F and Yan J: Inhibitory Effect of Neuropilin-1 monoclonal antibody (NRP-1 MAb) on glioma tumor in mice. J Biomed Nanotechnol 9: 551-558, 2013.
44. Dallas NA, Gray MJ, Xia L, Fan F, van Buren G II, Gaur P, Samuel S, Lim SJ, Arumugam T, Ramachandran V, *et al*: Neuropilin-2-mediated tumor growth and angiogenesis in pancreatic adenocarcinoma. Clin Cancer Res 14: 8052-8060, 2008.
45. Wang Y, Wang S, Ding Y, Ye Y, Xu Y, He H, Li Q, Mi Y, Guo C, Lin Z, *et al*: A suppressor of cytokine signaling 1 antagonist enhances antigen-presenting capacity and tumor cell antigen-specific cytotoxic T lymphocyte responses by human monocyte-derived dendritic cells. Clin Vaccine Immunol 20: 1449-1456, 2013.
46. Wu N, Wang Y, Wang S, Chen Y and Yan J: Recombinant human leptin induces growth inhibition and apoptosis in human gastric cancer MGC-803 cells. Clin Exp Med 13: 305-314, 2013.
47. Li YJ, Sun LC, He Y, Liu XH, Liu M, Wang QM and Jin XM: The anti-tumor properties of two tumstatin peptide fragments in human gastric carcinoma. Acta Pharmacologica Sinica 30: 1307-1315, 2009.
48. Cai Y, Wang R, Zhao YF, Jia J, Sun ZJ and Chen XM: Expression of Neuropilin-2 in salivary adenoid cystic carcinoma: Its implication in tumor progression and angiogenesis. Pathol Res Pract 206: 793-799, 2010.
49. Sulpice E, Plouët J, Bergé M, Allanic D, Tobelem G and Merkulova-Rainon T: Neuropilin-1 and neuropilin-2 act as coreceptors, potentiating proangiogenic activity. Blood 111: 2036-2045, 2008.
50. O'Reilly MS, Boehm T, Shing Y, Fukai N, Vasios G, Lane WS, Flynn E, Birkhead JR, Olsen BR and Folkman J: Endostatin: An endogenous inhibitor of angiogenesis and tumor growth. Cell 88: 277-285, 1997.
51. Zhang JL, Chen GW, Liu YC, Wang PY, Wang X, Wan YL, Zhu J, Gao HQ, Yin J, Wang W and Tian ML: Secreted protein acidic and rich in cysteine (SPARC) suppresses angiogenesis by down-regulating the expression of VEGF and MMP-7 in gastric cancer. PLoS One 7: e44618, 2012.
52. Xavier LL, Viola GG, Ferraz AC, Da Cunha C, Deonizio JM, Netto CA and Achaval M: A simple and fast densitometric method for the analysis of tyrosine hydroxylase immunoreactivity in the substantia nigra pars compacta and in the ventral tegmental area. Brain Res Brain Res Protoc 16: 58-64, 2005.
53. Fukahi K, Fukasawa M, Neufeld G, Itakura J and Korc M: Aberrant expression of neuropilin-1 and -2 in human pancreatic cancer cells. Clin Cancer Res 10: 581-590, 2004.
54. Stephenson JM, Banerjee S, Saxena NK, Cherian R and Banerjee SK: Neuropilin-1 is differentially expressed in myoepithelial cells and vascular smooth muscle cells in preneoplastic and neoplastic human breast: A possible marker for the progression of breast cancer. Int J Cancer 101: 409-414, 2002.
55. Lantuéjoul S, Constantin B, Drabkin H, Brambilla C, Roche J and Brambilla E: Expression of VEGF, semaphorin SEMA3F, and their common receptors neuropilins NP1 and NP2 in preinvasive bronchial lesions, lung tumours, and cell lines. J Pathol 200: 336-347, 2003.
56. Akagi M, Kawaguchi M, Liu W, McCarty MF, Takeda A, Fan F, Stoeltzing O, Parikh AA, Jung YD, Bucana CD, *et al*: Induction of neuropilin-1 and vascular endothelial growth factor by epidermal growth factor in human gastric cancer cells. Br J Cancer 88: 796-802, 2003.
57. Murga M, Fernandez-Capetillo O and Tosato G: Neuropilin-1 regulates attachment in human endothelial cells independently of vascular endothelial growth factor receptor-2. Blood 105: 1992-1999, 2005.
58. Manning BD and Cantley LC: AKT/PKB signaling: Navigating downstream. Cell 129: 1261-1274, 2007.
59. Engelman JA: Targeting PI3K signalling in cancer: Opportunities, challenges and limitations. Nat Rev Cancer 9: 550-562, 2009.
60. Burotto M, Chiou VL, Lee J-M and Kohn EC: The MAPK pathway across different malignancies: A new perspective. Cancer 120: 3446-3456, 2014.
61. Miao HQ, Lee P, Lin H, Soker S and Klagsbrun M: Neuropilin-1 expression by tumor cells promotes tumor angiogenesis and progression. FASEB J 14: 2532-2539, 2000.
62. Xia C, Meng Q, Ca Z, Shi X and Jiang B-H: Regulation of angiogenesis and tumor growth by p110 alpha and AKT1 via VEGF expression. J Cell Physiol 209: 56-66, 2006.
63. Mazure NM, Chen EY, Laderoute KR and Giaccia AJ: Induction of vascular endothelial growth factor by hypoxia is modulated by a phosphatidylinositol 3-kinase Akt signaling pathway in Ha-ras-transformed cells through a hypoxia inducible factor-1 transcriptional element. Blood 90: 3322-3331, 1997.
64. Zhong H, Chiles K, Feldser D, Laughner E, Hanrahan C, Georgescu MM, Simons JW and Semenza GL: Modulation of hypoxia-inducible factor 1 alpha expression by the epidermal growth factor/phosphatidylinositol 3-kinase/PTEN/AKT/FRAP pathway in human prostate cancer cells: Implications for tumor angiogenesis and therapeutics. Cancer Res 60: 1541-1545, 2000.
65. Jiang BH, Jiang G, Zheng JZ, Lu Z, Hunter T and Vogt PK: Phosphatidylinositol 3-kinase signaling controls levels of hypoxia-inducible factor. Cell Growth Differ 12: 363-369, 2001.
66. Skinner HD, Zheng JZ, Fang J, Agani F and Jiang BH: Vascular endothelial growth factor transcriptional activation is mediated by hypoxia-inducible factor 1 alpha, HDM2, and p70S6K1 in response to phosphatidylinositol 3-kinase/AKT signaling. J Biol Chem 279: 45643-45651, 2004.